

(19) World Intellectual Property Organization
International Bureau



(43) International Publication Date
22 October 2009 (22.10.2009)

PCT

(10) International Publication Number
WO 2009/127901 A1

- (51) **International Patent Classification:**
COIB 25/37 (2006.01) *HOIM* 4/62 (2006.01)
COIB 25/45 (2006.01)
- (21) **International Application Number:**
PCT/IB2008/05 1418
- (22) **International Filing Date:**
14 April 2008 (14.04.2008)
- (25) **Filing Language:** English
- (26) **Publication Language:** English
- (71) **Applicant (for all designated States except US):** **HIGH POWER LITHIUM S.A.** [CH/CH]; PSE-B EPFL, CH-101 5 Lausanne (CH).
- (72) **Inventor; and**
- (75) **Inventor/Applicant (for US only):** **KAY, Andreas** [-/CH]; Passage Bocion 5, CH- 1007 Lausanne (CH).
- (74) **Agent:** **ROLAND, Andre;** c/o ANDRE ROLAND S.A., P.O. Box 1255, CH-1001 Lausanne (CH).
- (81) **Designated States (unless otherwise indicated, for every kind of national protection available):** AE, AG, AL, AM,

AO, AT, AU, AZ, BA, BB, BG, BH, BR, BW, BY, BZ, CA, CH, CN, CO, CR, CU, CZ, DE, DK, DM, DO, DZ, EC, EE, EG, ES, FI, GB, GD, GE, GH, GM, GT, HN, HR, HU, ID, IL, IN, IS, JP, KE, KG, KM, KN, KP, KR, KZ, LA, LC, LK, LR, LS, LT, LU, LY, MA, MD, ME, MG, MK, MN, MW, MX, MY, MZ, NA, NG, NI, NO, NZ, OM, PG, PH, PL, PT, RO, RS, RU, SC, SD, SE, SG, SK, SL, SM, SV, SY, TJ, TM, TN, TR, TT, TZ, UA, UG, US, UZ, VC, VN, ZA, ZM, ZW.

(84) **Designated States (unless otherwise indicated, for every kind of regional protection available):** ARIPO (BW, GH, GM, KE, LS, MW, MZ, NA, SD, SL, SZ, TZ, UG, ZM, ZW), Eurasian (AM, AZ, BY, KG, KZ, MD, RU, TJ, TM), European (AT, BE, BG, CH, CY, CZ, DE, DK, EE, ES, FI, FR, GB, GR, HR, HU, IE, IS, IT, LT, LU, LV, MC, MT, NL, NO, PL, PT, RO, SE, SI, SK, TR), OAPI (BF, BJ, CF, CG, CI, CM, GA, GN, GQ, GW, ML, MR, NE, SN, TD, TG).

Published:
— with international search report (Art. 21(3))

(54) **Title:** LITHIUM METAL PHOSPHATE/CARBON NANOCOMPOSITES AS CATHODE ACTIVE MATERIALS FOR SECONDARY LITHIUM BATTERIES

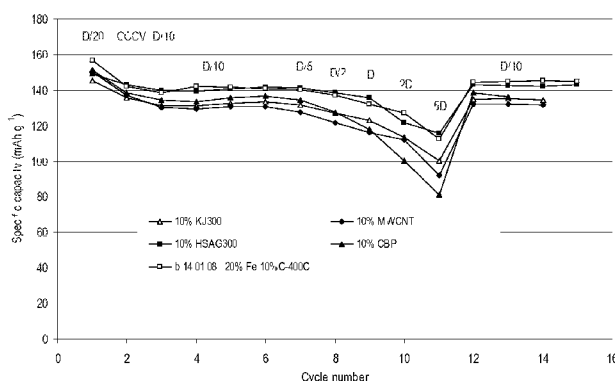


Figure 7

Electrochemical performance of lithium batteries with $\text{LiMn}_{0.5}\text{Fe}_{0.5}\text{PO}_4/\text{C}$ nanocomposite cathodes prepared from different carbon sources:

- Δ Ketjenblack EC-300J (Akzo Nobel, 800 m^2/g)
- Ketjenblack EC-600JD (Akzo Nobel, 1400 m^2/g)
- ▲ Black Pearls 2000 (Cabot, 1500 m^2/g)
- ◆ Multi walled carbon nanotubes (MWCNT)
- High surface graphite Timrex HSAG300 (Timcal, 280 m^2/g)

(57) **Abstract:** A lithium metal phosphate/carbon nanocomposite as cathode material for rechargeable electrochemical cells with the general formula $\text{Li}_x\text{M}_1\text{yM}_21\text{-yPO}_4/\text{C}$ where M_1 is Fe, Mn, Co, Ni, VF and M_2 is Fe, Mn, Co, Ni, VF, Mg, Ca, Al, B, Cr, Zn, Cu, Nb, Zr, V, Ti and $x = 0.8-1.0$ and $y = 0.5-1.0$, with a carbon content of 0.5 to 20% by weight.



WO 2009/127901 A1

LITHIUM METAL PHOSPHATE/CARBON
NANOCOMPOSITES AS CATHODE ACTIVE
MATERIALS FOR SECONDARY LITHIUM
5 BATTERIES

FIELD OF THE INVENTION

10

The invention relates to a lithium metal phosphate nanocomposite as cathode material for rechargeable electrochemical cells.

15

STATE OF THE ART

20

25

Rechargeable batteries of high energy density and long lifetime based on the reversible intercalation of lithium into certain materials have enabled the wide distribution of light and compact electronic devices, such as mobile phones and portable computers. However, the use of certain cathode materials, such as LiCoO_2 , has given rise to concerns because of the toxicity of cobalt and the danger of fire and explosion due to oxygen liberation and violent reaction with the organic electrolyte on overcharging or at elevated temperature (thermal runaway). Moreover cobalt is a rather rare and hence expensive element. Other materials, such as LiMn_2O_4 suffer from poor long term stability due to dissolution of Mn^{2+} in the electrolyte.

30

Lithium metal phosphates with olivine structure have emerged as a promising alternative as cathode materials, since the oxygen is strongly covalently bound in PO_4^{3-} , preventing the release of oxygen even under extreme conditions. In addition the inductive effect of PO_4^{3-} raises the redox potential of the metal centre, rendering the use of abundant and cheap metals

such as iron and manganese possible. Thus, LiFePO_4 yields a voltage of 3.4 V against lithium and remains stable over thousands of charge/discharge cycles, even upon overcharge and at elevated temperature. LiMnPO_4 gives an even higher voltage of 4.1 V against lithium, which is near the stability limit of common non-aqueous electrolytes and more compatible with classic systems, such as LiCoO_2 , $\text{LiAlO}_5\text{Co}_0.5\text{Ni}_0.8\text{O}_2$ or LiMn_2O_4 . Thanks to the higher voltage LiMnPO_4 offers a superior energy density to LiFePO_4 , which is important for many applications, especially battery electric vehicles.¹ However, only solid solutions $\text{LiMn}_y\text{Fe}_{1-y}\text{PO}_4$ were reported to be electrochemically active.²⁻⁴ Still, the capacity of $\text{LiMn}_{0.5}\text{Fe}_{0.5}\text{PO}_4$ was limited to 80 mAh/g, which is less than half the theoretical capacity of 169 mAh/g.

10

Almost full capacity has been reported for LiMnPO_4 and $\text{Li}_{1-x}\text{Mn}_y\text{Fe}_{1-y}\text{PO}_4$ prepared by ball milling of the precursors (MnCO_3 , $\text{FeC}_2\text{O}_4 \cdot 2\text{H}_2\text{O}$, $\text{NH}_4\text{H}_2\text{PO}_4$ and Li_2CO_3) with acetylene black and subsequent firing under inert gas atmosphere.⁵⁻¹⁶ It was claimed that this results in a grain size of $\text{Li}_{1-x}\text{Mn}_y\text{Fe}_{1-y}\text{PO}_4$ not larger than 10 μm , with the BET specific surface area not being less than 0.5 m^2/g .^{5, 6, 8-10, 15} At a carbon content of 10% and a current density of 0.28 mA/cm^2 a capacity of 164 mAh/g was reported for a Mn content of $y = 0.75$.¹⁶ Unfortunately, neither the charge/discharge rate nor the loading of active electrode material were indicated by the authors, but assuming a typical loading of 8 mg/cm^2 a current density of 0.28 mA/cm^2 corresponds to 35 mA/g, or a C-rate of C/5 (that is a charge/discharge time of 5 hours). Good capacity also at higher C-rate has not been reported for $\text{Li}_{1-x}\text{Mn}_y\text{Fe}_{1-y}\text{PO}_4$ so far, although this is essential for high power applications, such as hybrid or battery electric vehicles, in order to enable fast acceleration and battery recharging as well as efficient regenerative braking.

15

20

The poor electrochemical performance of LiMnPO_4 and $\text{LiMn}_y\text{Fe}_{1-y}\text{PO}_4$ has been attributed to their extremely low electronic and ionic conductivities.^{17, 18} Many efforts have therefore been undertaken to reduce the particle size to the sub-micrometer scale and coat such nanoparticles with conducting carbon, in order to diminish electric and Li-diffusion resistances by shortening the distances for electron and lithium transport.

25

30

Direct precipitation of LiMnPO_4 from aqueous medium produced particles down to about 100 nm, which after ball-milling with acetylene black gave reversible capacities of about 70 mAh/g at C/20.^{17, 19, 20} Hydrothermal synthesis of LiMnPO_4 produced platelets of 100-200 nm thickness, which after ball-milling with carbon black yielded a reversible capacity of 68 mAh/g at a current density of 1.5 mA/g.²¹ Solid-state synthesis of $\text{LiMn}_{0.6}\text{Fe}_{0.4}$ by ball-milling

followed by in situ carbon coating through pyrolysis of polypropylene produced 100-200 nm particles and an initial discharge capacity of 143 mAh/g at C/10.²² Sol-gel synthesis of LiMnPO_4 produced particles of 140-220 nm, which were reduced to 90-130 nm by ball-milling with acetylene black and yielded 134 mAh/g at C/10.²³⁻²⁵ Nanoparticles of LiMnPO_4 of 20-100 nm were obtained by a polyol process, which after ball-milling with acetylene black gave a capacity of about 120 mAh/g at C/10.²⁶ In conclusion good rate performance, i.e. high capacity at higher C-rates has still not been reported.

10

DESCRIPTION OF THE INVENTION

According to the present invention good capacity even at high C-rate is obtained with a nanocomposite of lithium metal phosphate LiMPO_4 and carbon, produced by milling of suitable precursors for LiMPO_4 with electro-conductive carbon black of high specific surface area, carbon nanotubes, graphite, expanded graphite or graphene. Milling breaks covalent bonds in the carbon material and creates highly reactive coordinatively unsaturated carbon atoms (dangling bonds) on the carbon surface with which the precursor for LiMPO_4 can react. This mechanochemical reaction²⁷⁻²⁹ results in a nanocomposite of LiMPO_4 precursors and carbon, wherein the size of the different domains can be controlled by the amount and type of carbon material as well as by the intensity and duration of milling. Thermal treatment leads to crystallization of LiMPO_4 already at relatively low temperature due to intimate mixing of the precursors by milling. This low crystallization temperature in combination with the covalently bound carbon prevents crystal growth and results in the small nanoparticle size of LiMPO_4 in intimate contact with conducting carbon required for good rate performance.

The metal M in LiMPO_4 may be Fe, Mn, Co, Ni or mixtures of these, as well as a mixture with other elements, such as Mg, Ca, Al, B, Cr, Zn, Cu, Nb, Ti, Zr, V. Part of the oxygen atoms O may be substituted by fluorine F or part of the phosphate ions PO_4^{3-} may be substituted by silicate ions SiO_4^{4-} or sulfate ions SO_4^{2-} .

Acetylene black is the only electro-conductive carbon for which the synthesis of LiMPO_4 / carbon composites by milling has been reported.^{5-9, 13-15, 30-34} Acetylene black has a BET specific surface area of only about 70 m²/g and consists of fused spherical primary particles

(nodules) of about 30 nm diameter with onion-shell structure of concentric graphene like outer layers, while the core is more amorphous.^{35' 36} The compactness and resilience of these nodules renders them rather resistant against breakdown by milling. This explains why acetylene black yields only poor rate performance (Figure 8).

5

Conductive carbon blacks with very specific surface area according to the present invention are for example the furnace blacks Printex XE 2 (Degussa) with 950 m²/g and fused carbon nodules of about 30 nm diameter, as well as Black Pearls 2000 (Cabot) with 1500 m²/g and 15 nm particle diameter. The much higher specific surface area as compared to acetylene black in spite of the similar nodule size is due to a more open, porous structure of these nodules, rendering them much more fragile against milling. Therefore milling not only breaks the chains of fused carbon nodules but also disrupts the graphene like shells of the nodules, creating dangling bonds for reaction with the LiMPO₄ precursors.

10

Ketjenblack (Akzo Nobel) is another conductive carbon black of high specific surface area (800-1400 m²/g). It is obtained as by-product in the synthesis of ammonia and has a fused broken egg-shell structure, which arises from removal of the inner amorphous part of the carbon black nodules by partial combustion.^{36' 37} These shells of about 20 nm outer diameters have a thickness of a few graphene layers only and thus are easily broken by milling.

20

Carbon nanotubes are single walled (SWCNT) or multi walled (MWCNT) tubes of enrolled graphene sheets, which exhibit very high specific surface area and can be broken by milling.

Graphitic nano-sheets can also be obtained by milling of graphite.³⁸⁻⁴⁹ Natural as well as synthetic graphite consists of stacked graphene sheets, which are bound by weak van der Waals forces only, and hence are easily separated by sheer forces during milling. This produces thinner graphene stacks which are more easily broken within the graphene planes by further milling, creating highly reactive dangling bonds at the freshly created edges. The milling time can be reduced by using expanded graphite, in which the graphene sheets have already been partially separated by chemical intercalation and thermal expansion. To reduce the milling time even further multiple or single sheet graphene can also be prepared by oxidation of graphite and subsequent exfoliation.⁵⁰

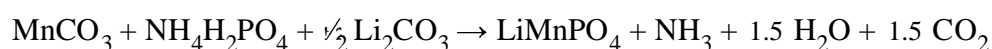
25

30

Breaking of carbon-carbon bonds by milling creates highly reactive coordinatively unsaturated carbon atoms (dangling bonds).⁵¹⁻⁵⁴ This freshly created carbon surface can react with the other precursors present in the mill (the amount of oxygen from the air contained in the closed milling vessel is relatively small and rapidly consumed by the carbon, so that its
5 removal by flushing with inert gas or evacuation is not necessary).

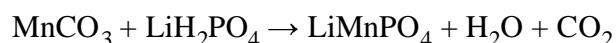
For the solid state synthesis of LiMnPO_4 by mechanochemical reaction the use of manganese(II)carbonate, ammonium di-hydrogen-phosphate and lithium carbonate has been reported:^{5-12, 16, 55}

10



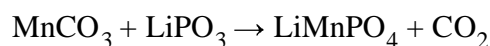
According to the present invention the liberation of toxic, corrosive and flammable NH_3 during milling can be avoided with lithium-di-hydrogen-phosphate:

15



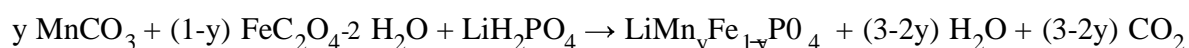
This also reduces the amount of water and carbon dioxide produced by 50%. Water as byproduct may be avoided completely by employing lithium metaphosphate:

20



Solid solutions with lithium iron phosphate can be obtained with e.g. iron oxalate:

25

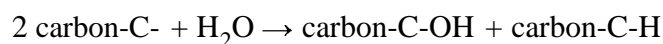


30

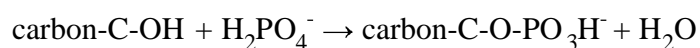
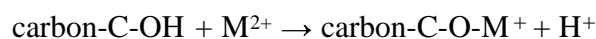
Other lithium metal phosphates and their solid solutions can be synthesized accordingly from the appropriate precursors. Instead of metal carbonates or oxalates any other suitable metal source can be used, such as oxides (e.g. MnO , Mn_2O_3 , MnO_2 , Fe_3O_4 , Fe_2O_3), hydroxides, salts with carboxylic acids (e.g. acetates) or hydroxyl carboxylic acids (e.g. glycolates, lactates, citrates, tartrates). Other lithium salts can be employed instead of LiH_2PO_4 or LiPO_3 , such as Li_2O , LiOH or Li_2CO_3 . Phosphate ions can also be introduced from phosphoric acid (H_3PO_4 or

H₃PO₄), as well as any phosphate salt, as long as the byproducts do not degrade the main product.

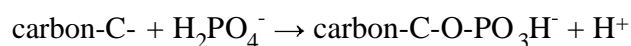
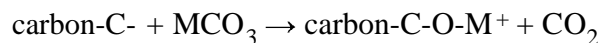
5 The water vapor produced by the mechanochemical reaction can dissociatively react with the freshly created carbon surface arising from disruption of carbon-carbon bonds by milling, resulting in a hydroxylation of the coordinatively unsaturated carbon atoms:



10 Subsequently these hydroxyl groups can react with transition metal or phosphate ions:



15 The coordinatively unsaturated carbon atoms created by milling can also react directly with the metal salt or phosphate ions:



20

Through these chemical reactions of the LiMPO₄ precursors with the carbon surface nucleation centers are created for the growth of covalently bound, amorphous LiMPO₄ by further mechanochemical reaction. On a carbon of very high specific surface area (as obtained
25 by milling with high surface area carbon black or graphite) the amorphous LiMPO₄ is very finely dispersed resulting in a nanocomposite of very small particle size after crystallization, which is crucial for good rate performance. Covalent binding of LiMPO₄ to carbon through oxygen bridges (C-O-M or C-O-P) also improves the electric contact of the cathode active material with the current collector of the battery, which again is important to achieve high
30 current densities. A stoichiometric excess of transition metal precursor during milling favors formation of a metal oxide bonding layer (C-O-M) between carbon and LiMPO₄, while an excess of phosphate favors bonding by phosphate groups (C-O-P).

The presence of covalent bonds between LiMPO_4 and carbon can be shown by different analytical techniques, such as infrared (FTIR) and Raman spectroscopy, or X-ray spectroscopy (e.g. XAFS, XANES, XPS). For example the formation of an intermediate manganese oxide bonding layer by ball-milling of nanocrystalline LiMnPO_4 with Ketjenblack in presence of a small amount of water has been revealed by Raman spectroscopy.⁵⁶

Due to the intimate mixing of the LiMPO_4 precursors by milling on the nanometer scale crystallization occurs already at moderate temperature (around 400°C). The low thermal diffusivity at such a low crystallization temperature results in the formation of very small nanocrystals. In addition, crystal growth is inhibited by the covalently bound carbon in the nanocomposite, which reduces the diffusivity even more. Hence a LiMPO_4 /carbon nanocomposite with nanocrystalline LiMPO_4 of less than about 100 nm crystallite size is formed and preserved after heat treatment at $350\text{-}600^\circ\text{C}$, resulting in high capacity at high C-rates. The primary particle size of LiMPO_4 in the nanocomposite can be determined by electron microscopy (SEM or TEM). The crystallite size of LiMPO_4 can be calculated from the X-ray diffraction line broadening with the Scherrer equation, or more accurately with the Warren-Averbach method, which takes into account the contribution of lattice strain to line broadening.

Up to about 300°C heating can occur in the presence of air until the reaction side products (mostly water and carbon dioxide with metal carbonate, metal oxalate and lithium-dihydrogen-phosphate precursors) are removed. Crystallization above 350°C requires an inert gas atmosphere to prevent, or at least a closed air space to limit the oxidation of carbon by oxygen.

The relative mass of carbon required to obtain an average carbon coating thickness t on spherical lithium metal phosphate particles of average radius r is given by:

$$M_{\text{carbon}}/M_{\text{LiMPO}_4} = \rho_{\text{carbon}}/\rho_{\text{LiMPO}_4} \cdot [(1+t/r)^3 - 1]$$

30

For $r=20$ nm and $t=1$ nm with $\rho_{\text{carbon}} = 2.2$ g/cm³ and $\rho_{\text{LiMPO}_4} = 3.5$ g/cm³:

$$M_{\text{carbon}}/M_{\text{LiMPO}_4} = 0.1$$

Hence for spherical LiMPO_4 particles of 40 nm average diameter and a continuous dense carbon coating of 1 nm mean thickness 10 wt% carbon with respect to the mass of LiMPO_4 would be required. The necessary amount would be higher for non-spherical particles since a sphere has the smallest surface area for a given volume. It would be lower for bigger LiMPO_4 particles or a thinner or discontinuous or less dense carbon coating.

Carbon exhibits good electric conductivity only in its graphite modification (sp^2 hybridized carbon) and only within the two-dimensional basal graphene planes. Hence for good electric conductivity of the carbon network in the nanocomposite a large fraction and sufficient extension of these graphitic domains with sp^2 carbon is required. Since the low heat treatment temperature of 350-600 $^{\circ}\text{C}$ is not sufficient to cause any graphitization a high graphene fraction must already be present in the carbon additive before milling. According to the present invention this is achieved by employing electro-conductive carbon black of high surface area, such as Printex XE 2 (Degussa), Black Pearls 2000 (Cabot) or Ketjenblack (Akzo Nobel), carbon nanotubes (SWCNT or MWCNT), graphite, expanded graphite or graphene. The fraction and size of well conducting graphene domains in the nanocomposite obtained by milling can be determined by different analytical techniques, such as Raman spectroscopy (ratio of graphene G-band around 1580 cm^{-1} and disorder D-band around 1360 cm^{-1})^{57, 58}, X-ray and neutron diffraction, as well as electron microscopy (TEM).

EXAMPLES

Example 1: Synthesis of LiMnPO_4/C nanocomposite

A mixture of 3.45 g MnCO_3 (Aldrich 99.9%) + 3.12 g LiH_2PO_4 (Aldrich 99%) + 1 g Ketjenblack EC600JD (Akzo Nobel) was milled in a hardened steel container of 250 mL capacity with 12 hardened steel balls of 20 mm diameter in a planetary ball mill (Retsch PM 100) at 500 rpm for 2 hours. The obtained powder was heated up to 450 $^{\circ}\text{C}$ within 30 minutes and maintained at this temperature for 1 hour under a stream of argon + 8% hydrogen.

Example 2: Synthesis of $\text{LiMn}_{0.9}\text{Fe}_0.1\text{PO}_4/\text{C}$ nanocomposite (18% Ketjenblack)

A mixture of 3.105 g MnCO_3 (Aldrich 99.9%) + 0.54 g $\text{FeC}_2\text{O}_4 \cdot 2 \text{H}_2\text{O}$ (Fluka 99%) + 3.12 g LiH_2PO_4 (Aldrich 99%) + 1 g Ketjenblack EC600JD was milled as described in Example 1 and heated at 350, 450 or 550°C for 1 hour under argon + 8% hydrogen.

Figure 1 shows a scanning electron microscope picture of the nanocomposite obtained at 450°C, indicating a primary particle size in the order of 50 nm for the brighter $\text{LiMn}_9\text{Fe}_1\text{PO}_4$ component.

Figure 2 shows the X-ray diffraction patterns of the three samples, indicating poor crystallization after 1 hour at 350°C, while the sample heated for the same time at 450°C is well crystallized $\text{LiMn}_9\text{Fe}_1\text{PO}_4$ without any apparent impurities. From the line broadening an average crystallite size of 60 nm with negligible strain was calculated with the Warren-Averbach method. This agrees with the primary particle size in the order of 50 nm observed in the SEM picture (Figure 1).

Example 3: Synthesis of $\text{LiMn}_8\text{Fe}_2\text{PO}_4/10\% \text{C}$ nanocomposites with different carbon materials

A mixture of 2.76 g MnCO_3 (Aldrich 99.9%) + 1.08 g $\text{FeC}_2\text{O}_4 \cdot 2 \text{H}_2\text{O}$ (Fluka 99%) + 3.12 g LiH_2PO_4 (Aldrich 99%) + 0.5 g carbon was milled and heat treated as described in Example 1.

Following carbon materials were compared:

Ketjenblack EC-300J (Akzo Nobel, 800 m^2/g)

Ketjenblack EC-600JD (Akzo Nobel, 1400 m^2/g)

Printex XE 2 (Degussa, 950 m^2/g)

Black Pearls 2000 (Cabot, 1500 m^2/g)

Shawinigan acetylene black C-55 (70 m^2/g)

Multi walled carbon nanotubes (MWCNT)

High surface graphite Timrex HSAG300 (Timcal, 280 m^2/g)

Timrex KS4 graphite (Timcal, 26 m^2/g)

Timrex KS6 graphite (Timcal, 20 m^2/g)

Timrex SFG6 graphite (Timcal, 17 m^2/g)

Timrex MB 15 graphite (Timcal, 9.5 m^2/g)

Example 4: Synthesis of $\text{LiFePO}_4/3\% \text{C}$ nanocomposite

5

A mixture of 5.4 g $\text{FeC}_2\text{O}_4 \cdot 2 \text{H}_2\text{O}$ + 3.12 g LiH_2PO_4 + 0.15 g SFG6 graphite (Timcal) was milled and heat treated as described in Example 1.

10 **Example 5:** Synthesis of $\text{LiFe}_{0.9}\text{Mn}_{0.1}\text{PO}_4/3\% \text{C}$ nanocomposite

A mixture of 4.86 g $\text{FeC}_2\text{O}_4 \cdot 2 \text{H}_2\text{O}$ + 0.345 g MnCO_3 + 3.12 g LiH_2PO_4 + 0.15 SFG6 graphite (Timcal) was milled and heat treated as described in Example 1.

15 **Example 6:** Preparation of a $\text{LiMn}_y\text{Fe}_{1-y}\text{PO}_4/\text{C}$ cathodes and secondary lithium batteries with such cathodes

1 g of $\text{LiMn}_y\text{Fe}_{1-y}\text{PO}_4/\text{C}$ nanocomposite as obtained in Example 1 to 5 was mixed with 20 mg graphite powder and 75 mg PVdF (polyvinylidene difluoride) in NMP (N-methyl-2-pyrrolidinon). This dispersion was doctor bladed on a carbon coated aluminum foil and dried at 120°C under vacuum. The electrodes were compressed into 0.23 mm disks with a thickness of about 30 μm and an active material loading of about 3.0 mg/cm^2 . Cells were assembled in SwagelokTM fittings using Li metal foil as counter electrode with a microporous polymer separator (Celgard 2400TM) and an electrolyte of 1M LiPF_6 in propylene carbonate (PC), ethylene carbonate (EC) and dimethyl carbonate (DMC) (1:1:3 by volume). The electrochemical properties of the $\text{LiMn}_y\text{Fe}_{1-y}\text{PO}_4/\text{C}$ electrodes were measured by galvanostatic charge/discharge and cyclic voltammetry with Arbin BT 2000. Figures 3, 5, 7 and 8 show the electrochemical performance at different discharging rates. Figures 4 and 6 show the stability on cycling at a charge/discharge rate of 1 C.

30

BRIEF DISCRIPTION OF THE DRAWINGS

5

Figure 1 shows a scanning electron microscope (SEM) picture of the $\text{LiMn}_{0.9}\text{Fe}_0.1\text{PO}_4/\text{C}$ nanocomposite (18% Ketjenblack EC600JD) according to Example 2 after heating for 1 hour under argon/8% hydrogen at 450°C . The primary particle size is in the order of 50 nm for the brighter $\text{LiMn}_{0.9}\text{Fe}_0.1\text{PO}_4$ component.

10

Figure 2 shows the X-ray diffraction (XRD) patterns of the $\text{LiMn}_{0.9}\text{Fe}_0.1\text{PO}_4/\text{C}$ nanocomposite (18% Ketjenblack EC600JD) according to Example 2 after heating for 1 hour under argon/8% hydrogen at different temperatures. Only weak XRD peaks are observed after 1 hour at 350°C indicating poor crystallization, while the sample heated for the same time at 450°C is well crystallized $\text{LiMn}_{0.9}\text{Fe}_0.1\text{PO}_4$ without any apparent impurities. Heating at 550°C leads to a further increase in the peak intensities and slight reduction in the peak widths. From the line broadening at 450°C an average crystallite size of 60 nm with negligible strain was calculated with the Warren-Averbach method. This agrees with the primary particle size in the order of 50 nm observed in the SEM picture (Figure 1).

20

Figure 3 represents the electrochemical performance of two different lithium batteries with $\text{LiMn}_{0.9}\text{Fe}_0.1\text{PO}_4/\text{C}$ nanocomposite cathode (18% Ketjenblack EC600JD) at different discharge rates on cycling between 2.7 and 4.4 V against lithium. A capacity of 150 mAh/g of active material is achieved at D/10. Even at a discharge rate of 5D a capacity as high as 130

25

mAh/g is obtained.

Figure 4 shows the cycling stability (at 1 C and C/10 each 10th cycle, charged up to 4.25 V) of the lithium batteries from Figure 3 with $\text{LiMn}_{0.9}\text{Fe}_0.1\text{PO}_4/\text{C}$ nanocomposite cathode (18% Ketjenblack EC600JD).

30

Figure 5 shows the electrochemical performance of a lithium battery with $\text{LiMn}_{0.9}\text{Fe}_0.1\text{PO}_4/\text{C}$ nanocomposite cathode (10% Ketjenblack EC600JD) at different discharge rates on cycling between 2.7 and 4.4 V against lithium. A capacity of 145 mAh/g of active material is obtained at D/10. At a discharge rate of 5D the capacity is still higher than 110 mAh/g.

Figure 6 shows the cycling stability (at 1 C and C/10 each 10th cycle, charged up to 4.25 V) of two lithium batteries according to Figure 5 with $\text{LiMn}_0.8\text{Fe}_{0.2}\text{PO}_4/\text{C}$ nanocomposite cathode (10% Ketjenblack EC600JD).

5

Figure 7 shows the electrochemical performance of lithium batteries with $\text{LiMn}_0.8\text{Fe}_{0.2}\text{PO}_4/10\%\text{C}$ nanocomposite cathodes prepared from different carbon sources on cycling between 2.7 and 4.4 V against lithium:

△ Ketjenblack EC-300J (Akzo Nobel, 800 m²/g)

10 a Ketjenblack EC-600JD (Akzo Nobel, 1400 m²/g)

▲ Black Pearls 2000 (Cabot, 1500 m²/g)

◆ Multi walled carbon nanotubes (MWCNT)

■ High surface graphite Timrex HSAG300 (Timcal, 280 m²/g)

15 Ketjenblack EC-600JD and high surface graphite Timrex HSAG300 show the best performance with a capacity of 145 mAh/g at D/10 and more than 110 mAh/g at 5D.

Figure 8 shows the electrochemical performance of lithium batteries with $\text{LiMn}_0.8\text{Fe}_{0.2}\text{PO}_4/10\%\text{C}$ nanocomposite cathodes prepared from different carbon sources on cycling between 2.7 and 4.4 V against lithium:

20 A Ketjenblack EC-600JD (Akzo Nobel, 1400 m²/g)

◆ Timrex KS4 graphite (Timcal, 26 m²/g)

0 Timrex SFG6 graphite (Timcal, 17 m²/g)

a Timrex MB 15 graphite (Timcal, 9.5 m²/g)

△ Shawinigan acetylene black C-55 (70 m²/g)

25 The three different graphites yield comparable performance to Ketjenblack EC-600JD. Shawinigan acetylene black C-55 gives much lower capacity, especially at higher discharge rates.

REFERENCES

- I. Howard, W. F.; Spotnitz, R. M., Theoretical evaluation of high-energy lithium metal phosphate cathode materials in Li-ion batteries. *Journal of Power Sources* **2007**, 165, (2), 887-891.<http://dx.doi.org/10.1016/j.jpowsour.2006.12.046>
- 5 2. Padhi, A. K.; Nanjundaswamy, K. S.; Goodenough, J. B., Phospho-olivines as positive-electrode materials for rechargeable lithium batteries. *Journal of the Electrochemical Society* 1997, 144, (4), 1188-1194.<http://dx.doi.org/10.1149/1.1837571>
3. Goodenough, J. B., Cathode materials for secondary (rechargeable) lithium batteries. *US5910382* 1999.<http://www.google.com/patents?id=RYEZAAAEB AJ&dq=goodenough>
- 10 4. Goodenough, J. B., Cathode materials for secondary (rechargeable) lithium batteries. *US6514640* 2003.<http://www.google.com/patents?id=L4NAAAEB AJ&dq=goodenough>
5. Yamada, A.; Li, G.; Azuma, H., Positive electrode active material, non-aqueous electrolyte secondary battery. *US7217474* 2007.http://www.google.com/patents?id=BPh_AAAEB AJM q=7217474
- 15 6. Yamada, A.; Li, G.; Azuma, H., Positive electrode active material, non-aqueous electrolyte secondary battery. *US7147969* 2006.<http://www.google.com/patents?id=oJd9AAAEB AJ&dq=7147969>
7. Okawa, T.; Hosoya, M.; Kuyama, J.; Fukushima, Y., Non-aqueous electrolyte secondary cell with a lithium metal phosphate cathode. *US7122272* 2006.<http://www.google.com/patents?id=dhh7AAAEB AJ&dq=7122272>
- 20 8. Li, G., Positive electrode material and battery using the same. *US7029795* 2006.<http://www.google.com/patents?id=M^AoN3AAAEB AJ&dq=7029795>
9. Li, G., Positive electrode active material and non-aqueous electrolyte cell. *US6749967* 2004.<http://www.google.com/patents?id=8fAPAAAEB AJ&dq=6749967>
- 25 <http://www.freepatentsonline.com/6749967.html>
10. Yamada, A.; Li, G.; Azuma, H., Positive electrode active material, non-aqueous electrolyte secondary battery. *US6632566* 2003.<http://www.google.com/patents?id=t58NAAAEB AJ&dq=Guohua+Li>
- II. Li, G. H.; Azuma, H.; Tohda, M., LiMnPO₄ as the cathode for lithium batteries. *Electrochemical and Solid State Letters* **2002**, 5, (6), A135-A137.<http://dx.doi.org/10.1149/1.1475195>
- 30 12. Yamada, A.; Chung, S. C., Crystal chemistry of the olivine-type Li(MnyFel-y)PO₄ and (MnyFel-y)PO₄ as possible 4 V cathode materials for lithium batteries. *Journal of the Electrochemical Society* **2001**, 148, (8), A960-A967. <http://dx.doi.org/10.1149/1.1385377>
- 35 13. Yamada, A.; Hosoya, M.; Chung, S. C.; Kudo, Y.; Hinokuma, K.; Liu, K. Y.; Nishi, Y., Olivine-type cathodes achievements and problems. *Journal of Power Sources* **2003**, 119, 232-238.[http://dx.doi.org/10.1016/S0378-7753\(03\)00239-8](http://dx.doi.org/10.1016/S0378-7753(03)00239-8)
14. Li, G.; Yamada, A.; Azuma, H., Method for manufacturing active material of positive plate and method for manufacturing nonaqueous electrolyte secondary cell. *EP1094532* **2001**,
- 40 15. Li, G.; Yamada, A., Positive electrode active material and non-aqueous electrolyte cell. *US20010055718* 2001.<http://www.freepatentsonline.com/ti/20010055718.html>
16. Li, G. H.; Azuma, H.; Tohda, M., Optimized LiMnyFel-yPO₄ as the cathode for lithium batteries. *Journal of the Electrochemical Society* **2002**, 149, (6), A743-A747. <http://dx.doi.org/10.1149/1.1473776>
- 45 17. Delacourt, C.; Laffont, L.; Bouchet, R.; Wurm, C.; Leriche, J. B.; Morcrette, M.; Tarascon, J. M.; Masquelier, C., Toward understanding of electrical limitations (electronic, ionic) in LiMPO₄ (M = Fe, Mn) electrode materials. *Journal of the Electrochemical Society* 2005, 152, A913-A921. <http://dx.doi.org/10.1149/1.1884787>

18. Molenda, J.; Ojczyk, W.; Marzec, J., Electrical conductivity and reaction with lithium of LiFe_{1-y}Mn_yPO₄ olivine-type cathode materials. *Journal of Power Sources* **2007**, 174, (2), 689-694.<http://dx.doi.org/10.1016/j.jpowsour.2007.06.238>
19. Delacourt, C ; Poizot, P.; Morcrette, M.; Tarascon, J. M.; Masquelier, C , One-step low-temperature route for the preparation of electrochemically active LiMnPO₄ powders. *Chemistry of Materials* **2004**, 16, (1), 92-99.<http://dx.doi.org/10.1021/cm030347b>
20. Delacourt, C ; Wurm, C ; Reale, P.; Morcrette, M.; Masquelier, C , Low temperature preparation of optimized phosphates for Li-battery applications. *Solid State Ionics* **2004**, 173, (1-4), 113-118.<http://dx.doi.org/10.1016/j.ssi.2004.07.061>
21. Fang, H. S.; Li, L. P.; Li, G. S., Hydrothermal synthesis of electrochemically active LiMnPO₄. *Chemistry Letters* **2007**, 36, 436-437.<Go to ISI>://WOS:000246058000043
22. Mi, C. H.; Zhang, X. G.; Zhao, X. B.; Li, H. L., Synthesis and performance of LiMnO₆FeO₄PO₄/nano-carbon webs composite cathode. *Materials Science and Engineering B-Solid State Materials for Advanced Technology* **2006**, 129, (1-3), 8-13.<http://dx.doi.org/10.1016/j.mseb.2005.11.015>
23. Drezen, T.; Kwon, N.-H.; Bowen, P.; Teerlinck, L; Isono, M.; Exnar, L, Effect of particle size on LiMnPO₄ cathodes. *Journal of Power Sources* **2007**, 174, (2), 949-953.<http://dx.doi.org/10.1016/j.jpowsour.2007.06.203>
24. Kwon, N. H.; Drezen, T.; Exnar, L; Teerlinck, L; Isono, M.; Graetzel, M., Enhanced electrochemical performance of mesoparticulate LiMnPO₄ for lithium ion batteries. *Electrochemical and Solid State Letters* **2006**, 9, (6), A277-A280.<http://dx.doi.org/10.1149/1.2221919>
25. KWON ROTH, N. H., Mesoscopic manganese based cathode materials for high voltage lithium ion batteries. *Ph.D. Thesis, ÉCOLE POLYTECHNIQUE FÉDÉRALE DE LA USANNE* **2006**.<http://library.epfl.ch/theses/?nP=3502>
26. Exnar, L; Drezen, T., Synthesis of nanoparticles of lithium metal phosphate positive material for lithium secondary battery. *PCT/IB2006/051061* **2006**.<http://www.wipo.int/pctdb/en/wo.jsp?wo=2Q07113624>
27. Boldyrev, V. V., Mechanochemistry and mechanical activation of solids. *Russian Chemical Reviews* **2006**, 75, (3), 177-189.<http://dx.doi.org/10.1070/RC2006v075n03ABEH001205>
28. Suryanarayana, C , *Mechanical Alloying and Milling*. Marcel Dekker: New York, 2004.
29. Tarascon, J. M.; Morcrette, M.; Saint, J.; Aymard, L.; Janot, R., On the benefits of ball milling within the field of rechargeable Li-based batteries. *Comptes Rendus Chimie* **2005**, 8, (1), 17-26.<http://dx.doi.org/10.1016/j.crci.2004.12.006>
30. Hosoya, M.; Takahashi, K.; Fukushima, Y., Cathode active material, method for preparation thereof, non-aqueous electrolyte cell and method for preparation thereof. *EP1184920* 2002.<http://www.freepatentsonline.com/EP1184920.html>
31. Hosoya, M.; Takahashi, K.; Fukushima, Y., Method for the preparation of cathode active material and method for the preparation of a non-aqueous electrolyte cell. *EPI 193783* 2002.<http://www.freepatentsonline.com/EPI193783.html>
32. Hosoya, M.; Takahashi, K.; Fukushima, Y., Method for the preparation of cathode active material and method for the preparation of a non-aqueous electrolyte cell. *EPI 193784* 2002.<http://www.freepatentsonline.com/EPI193784.html>
33. Hosoya, M.; Takahashi, K.; Fukushima, Y., Method for the preparation of cathode active material and method for the preparation of a non-aqueous electrolyte cell. *EP1193786* 2007.<http://www.freepatentsonline.com/EPI193786.html>

34. Hosoya, M.; Takahashi, K.; Fukushima, Y., Method for the preparation of cathode active material and method for the preparation of a non-aqueous electrolyte cell. *EPI 193787* 2002.<http://www.freepatentsonline.com/EPI193787.html>
<http://v3.espacenet.com/textdoc?DB=EPODOC&IDX=KR20020025819>
- 5 35. Ozawa, M.; Osawa, E., *Carbon Blacks as the Source Materials for Carbon*, in "Carbon Nanotechnology", Dai, L. (Ed.), Chapt. 6, p. 127-151, Elsevier: Dordrecht, 2006. 2006.
36. Tashima, D.; Kurosawatsu, K.; Uota, M.; Karashima, T.; Sung, Y. M.; Otsubo, M.; Honda, C., Space charge behaviors of electric double layer capacitors with nanocomposite electrode. *Surface & Coatings Technology* 2007, 201, (9-11), 5392-5395.<http://dx.doi.org/10.1016/j.surfcoat.2006.07.045>
- 10 37. Nelson, J. R.; Wissing, W. K., Morphology of Electrically Conductive Grades of Carbon-Black. *Carbon* 1986, 24, (2), 115-121.[http://dx.doi.org/10.1016/0008-4221\(86\)90104-1](http://dx.doi.org/10.1016/0008-4221(86)90104-1)
- 15 38. Antisari, M. V.; Montone, A.; Jovic, N.; Piscopiello, E.; Alvani, C.; Pilloni, L., Low energy pure shear milling: A method for the preparation of graphite nano-sheets. *Scripta Materialia* 2006, 55, (11), 1047-1050.<http://dx.doi.org/10.1016/j.scriptamat.2006.08.002>
39. Wong, S. C.; Sutherland, E. M.; Uhl, F. M., Materials processes of graphite nanostructured composites using ball milling. *Materials and Manufacturing Processes* 2006, 20, (2), 159-166.<http://dx.doi.org/10.1081/AMP-200068659>
- 20 40. Drogenik, M.; Makovec, D.; Kosak, A.; Kristl, M., Synthesis of carbon nanostructures with mechanical alloying. *Progress in Advanced Materials and Processes* 2004, 453-454, 213-217.<http://scholar.google.com/scholar?Mq=&lr=&cluster=12937135160538548640>
41. Chen, X. H.; Yang, H. S.; Wu, G. T.; Wang, M.; Deng, F. M.; Zhang, X. B.; Peng, J. C.; Li, W. Z., Generation of curved or closed-shell carbon nanostructures by ball-milling of graphite. *Journal of Crystal Growth* 2000, 218, (1), 57-61.[http://dx.doi.org/10.1016/S0022-0248\(00\)00486-3](http://dx.doi.org/10.1016/S0022-0248(00)00486-3)
- 25 42. Chen, Y.; Fitz Gerald, J. D.; Chadderton, L. T.; Chaffron, L., Nanoporous carbon produced by ball milling. *Applied Physics Letters* 1999, 74, (19), 2782-2784.<http://dx.doi.org/10.1063/U24012>
- 30 43. Huang, J. Y.; Yasuda, H.; Mori, H., Highly curved carbon nanostructures produced by ball-milling. *Chemical Physics Letters* 1999, 303, (1-2), 130-134.[http://dx.doi.org/10.1016/S0009-2614\(99\)00131-1](http://dx.doi.org/10.1016/S0009-2614(99)00131-1)
44. Harker, H.; Horsley, J. B.; Robson, D., Active Centres Produced in Graphite by Powdering. *Carbon* 1971, 9, (1), 1-8.[http://dx.doi.org/10.1016/0008-6223\(71\)90139-4](http://dx.doi.org/10.1016/0008-6223(71)90139-4)
- 35 45. Hentsche, M.; Hermann, H.; Gemming, T.; Wendrock, H.; Wetzig, K., Nanostructured graphite prepared by ball-milling at low temperatures. *Carbon* 2006, 44, (4), 812-814.<http://dx.doi.org/10.1016/j.carbon.2005.10.037>
46. Salver-Disma, F.; Tarascon, J. M.; Clinard, C.; Rouzaud, J. N., Transmission electron microscopy studies on carbon materials prepared by mechanical milling. *Carbon* 1999, 37, (12), 1941-1959.[http://dx.doi.org/10.1016/S0008-6223\(99\)00059-7](http://dx.doi.org/10.1016/S0008-6223(99)00059-7)
- 40 47. Janot, R.; Guerard, D., Ball-milling: the behavior of graphite as a function of the dispersal media. *Carbon* 2002, 40, (15), 2887-2896.[http://dx.doi.org/10.1016/S0008-6223\(02\)00223-3](http://dx.doi.org/10.1016/S0008-6223(02)00223-3)
- 45 48. Ong, T. S.; Yang, H., Effect of atmosphere on the mechanical milling of natural graphite. *Carbon* 2000, 38, (15), 2077-2085.[http://dx.doi.org/10.1016/S0008-6223\(00\)00064-6](http://dx.doi.org/10.1016/S0008-6223(00)00064-6)
49. Salver-Disma, F.; Du Pasquier, A.; Tarascon, J. M.; Lassegues, J. C.; Rouzaud, J. N., Physical characterization of carbonaceous materials prepared by mechanical grinding. *Journal of Power Sources* 1999, 82, 291-295.[http://dx.doi.org/10.1016/S0378-7753\(99\)00205-0](http://dx.doi.org/10.1016/S0378-7753(99)00205-0)
- 50

50. Geim, A. K.; Novoselov, K. S., The rise of graphene. *Nature Materials* **2007**, 6, (3), 183-191.<Go to ISI>://000244570700015
51. Jiang, D. E.; Sumpter, B. G.; Dai, S., Unique chemical reactivity of a graphene nanoribbon's zigzag edge. *Journal of Chemical Physics* **2007**, 126, (13).<http://dx.doi.org/10.1063/1.2715558>
52. Enoki, T.; Kobayashi, Y.; Fukui, K. L., Electronic structures of graphene edges and nanographene. *International Reviews in Physical Chemistry* **2007**, 26, 609-645.<http://dx.doi.org/10.1080/01442350701611991>
53. Hermann, H.; Schubert, T.; Gruner, W.; Mattern, N., Structure and chemical reactivity of ball-milled graphite. *Nanostructured Materials* **1997**, 8, (2), 215-229.[http://dx.dui.org/10.1016/S\(965-9773\(97\)10001\(0\)-X](http://dx.dui.org/10.1016/S(965-9773(97)10001(0)-X)
54. Francke, M.; Hermann, H.; Wenzel, R.; Seifert, G.; Wetzig, K., Modification of carbon nanostructures by high energy ball-milling under argon and hydrogen atmosphere. *Carbon* **2005**, 43, (6), 1204-1212.<http://dx.doi.org/10.1016/j.carbon.2004.12.013>
55. Li, G. H.; Kudo, Y.; Liu, K. Y.; Azuma, H.; Tohda, M., X-ray absorption study of $\text{Li}_x\text{MnyFel-yPO}_4$ ($0 \leq x \leq 1, 0 \leq y \leq 1$). *Journal of the Electrochemical Society* **2002**, 149, (11), A1414-A1418.<http://dx.doi.org/10.1149/1.1510768>
56. Exnar, L.; Drezen, T.; Frank; Zukalova; Miners, J.; Kavan, L., Carbon Coated Lithium Manganese Phosphate Cathode Material. *EPA No. 07112490.3*,
57. Tuinstra, F.; Koenig, J. L., Raman Spectrum of Graphite. *Journal of Chemical Physics* **1970**, 53, (3), 1126-&. <http://dx.doi.org/10.1063/1.1674108>
58. Nakamizo, M.; Honda, H.; Inagaki, M., Raman spectra of ground natural graphite. *Carbon* **1978**, 16, (4), 281-283.[http://dx.doi.org/10.1016/0008-6223\(78\)90043-X](http://dx.doi.org/10.1016/0008-6223(78)90043-X)

5

CLAIMS

- 10 1. A lithium metal phosphate/carbon nanocomposite as cathode material for rechargeable electrochemical cells with the general formula $\text{Li}_x\text{M1}_y\text{M2}_{1-y}\text{PO}_4/\text{C}$ where M1 is Fe, Mn, Co, Ni, VF and M2 is Fe, Mn, Co, Ni, VF, Mg, Ca, Al, B, Cr, Zn, Cu, Nb, Zr, V, Ti and $x = 0.8-1.0$ and $y = 0.5-1.0$, with a carbon content of 0.5 to 20% by weight.
- 15 2. A lithium metal phosphate/carbon nanocomposite according to claim 1, wherein the average crystallite size of the $\text{Li}_x\text{M1}_y\text{M2}_{1-y}\text{PO}_4$ domains as determined by X-ray diffraction is not larger than 300 nm.
- 20 3. A lithium metal phosphate/carbon nanocomposite according to claim 1, wherein the average crystallite size of the $\text{Li}_x\text{M1}_y\text{M2}_{1-y}\text{PO}_4$ domains as determined by X-ray diffraction is not larger than 200 nm.
- 25 4. A lithium metal phosphate/carbon nanocomposite according to claim 1, wherein the average crystallite size of the $\text{Li}_x\text{M1}_y\text{M2}_{1-y}\text{PO}_4$ domains as determined by X-ray diffraction is not larger than 100 nm.
- 30 5. A lithium metal phosphate/carbon nanocomposite according to claim 1, wherein the average crystallite size of the $\text{Li}_x\text{M1}_y\text{M2}_{1-y}\text{PO}_4$ domains as determined by X-ray diffraction is not larger than 80 nm.
6. A lithium metal phosphate/carbon nanocomposite according to claim 1, wherein the average crystallite size of the $\text{Li}_x\text{M1}_y\text{M2}_{1-y}\text{PO}_4$ domains as determined by X-ray diffraction is not larger than 60 nm.

7. A lithium metal phosphate/carbon nanocomposite according to claim 1, wherein the average crystallite size of the $\text{Li}_x\text{M1}_y\text{M2}_{1-y}\text{PO}_4$ domains as determined by X-ray diffraction is not larger than 50 nm.
- 5
8. A lithium metal phosphate/carbon nanocomposite according to claim 1, wherein the average crystallite size of the $\text{Li}_x\text{M1}_y\text{M2}_{1-y}\text{PO}_4$ domains as determined by X-ray diffraction is not larger than 40 nm.
- 10
9. A lithium metal phosphate/carbon nanocomposite according to claim 1, wherein the average cross-sectional dimension of the $\text{Li}_x\text{M1}_y\text{M2}_{1-y}\text{PO}_4$ domains as determined by electron microscopy is not larger than 300 nm.
10. A lithium metal phosphate/carbon nanocomposite according to claim 1, wherein the average cross-sectional dimension of the $\text{Li}_x\text{M1}_y\text{M2}_{1-y}\text{PO}_4$ domains as determined by electron microscopy is not larger than 200 nm.
- 15
11. A lithium metal phosphate/carbon nanocomposite according to claim 1, wherein the average cross-sectional dimension of the $\text{Li}_x\text{M1}_y\text{M2}_{1-y}\text{PO}_4$ domains as determined by electron microscopy is not larger than 100 nm.
- 20
12. A lithium metal phosphate/carbon nanocomposite according to claim 1, wherein the average cross-sectional dimension of the $\text{Li}_x\text{M1}_y\text{M2}_{i-y}\text{PO}_4$ domains as determined by electron microscopy is not larger than 80 nm.
- 25
13. A lithium metal phosphate/carbon nanocomposite according to claim 1, wherein the average cross-sectional dimension of the $\text{Li}_x\text{M1}_y\text{M2}_{i-y}\text{PO}_4$ domains as determined by electron microscopy is not larger than 60 nm.
- 30
14. A lithium metal phosphate/carbon nanocomposite according to claim 1, wherein the average cross-sectional dimension of the $\text{Li}_x\text{M1}_y\text{M2}_{i-y}\text{PO}_4$ domains as determined by electron microscopy is not larger than 50 nm.

15. A lithium metal phosphate/carbon nanocomposite according to claim 1, wherein the average cross-sectional dimension of the $\text{Li}_x\text{MI}_y\text{M}_{2-1-y}\text{PO}_4$ domains as determined by electron microscopy is not larger than 40 nm.
- 5 16. A lithium metal phosphate/carbon nanocomposite according to claims 1 to 15, wherein the integrated peak intensity ratio $R = \text{D/G}$ of the D-band around 1360 cm^{-1} and the G-band around 1580 cm^{-1} in the Raman spectrum due to disordered and graphene carbon is not larger than 1.0. (comment: Sony claims the opposite: D/G not smaller than 0.3, but for the precursor carbon material, not the product).^{7, 30-34}
- 10 17. A lithium metal phosphate/carbon nanocomposite according to claims 1 to 15, wherein the integrated peak intensity ratio $R = \text{D/G}$ of the D-band around 1360 cm^{-1} and the G-band around 1580 cm^{-1} in the Raman spectrum due to disordered and graphene carbon is not larger than 0.8.
- 15 18. A lithium metal phosphate/carbon nanocomposite according to claims 1 to 15, wherein the integrated peak intensity ratio $R = \text{D/G}$ of the D-band around 1360 cm^{-1} and the G-band around 1580 cm^{-1} in the Raman spectrum due to disordered and graphene carbon is not larger than 0.6.
- 20 19. A lithium metal phosphate/carbon nanocomposite according to claims 1 to 15, wherein the integrated peak intensity ratio $R = \text{D/G}$ of the D-band around 1360 cm^{-1} and the G-band around 1580 cm^{-1} in the Raman spectrum due to disordered and graphene carbon is not larger than 0.5.
- 25 20. A lithium metal phosphate/carbon nanocomposite according to claims 1 to 15, wherein the integrated peak intensity ratio $R = \text{D/G}$ of the D-band around 1360 cm^{-1} and the G-band around 1580 cm^{-1} in the Raman spectrum due to disordered and graphene carbon is not larger than 0.4.
- 30 21. A lithium metal phosphate/carbon nanocomposite according to claims 1 to 15, wherein the integrated peak intensity ratio $R = \text{D/G}$ of the D-band around 1360 cm^{-1} and the G-band around 1580 cm^{-1} in the Raman spectrum due to disordered and graphene carbon is not larger than 0.3.

22. A lithium metal phosphate/carbon nanocomposite according to claims 1 to 21, wherein the carbon is covalently bound to the lithium metal phosphate through carbon-oxygen-metal (C-O-M) and/or carbon-oxygen-phosphor (C-O-P) bridges.
23. A lithium metal phosphate/carbon nanocomposite according to claims 1 to 22, wherein M1 = Mn and M2 = Fe.
24. A lithium metal phosphate/carbon nanocomposite according to claims 1 to 22, wherein M1 = Fe and M2 = Mn.
25. A lithium metal phosphate/carbon nanocomposite according to claims 1 to 22, wherein M1 = M2 = Fe.
26. A process for the production of lithium metal phosphate/carbon nanocomposites according to claims 1 to 25, in which the precursors for the lithium metal phosphate are milled with a carbon material and subsequently heated for crystallization.
27. A process for the production of lithium metal phosphate/carbon nanocomposites according to claim 26, in which the metal precursors for lithium metal phosphate are metal carbonates or oxalates or oxides (e.g. MnO, Mn₂O₃, MnO₂, Fe₃O₄, Fe₂O₃), hydroxides, salts with carboxylic acids (e.g. acetates) or hydroxyl carboxylic acids (e.g. glycolates, lactates, citrates, tartrates), or any other metal compound that produces no byproducts which degrade the main product.
28. A process for the production of lithium metal phosphate/carbon nanocomposites according to claim 26, in which the lithium precursor for lithium metal phosphate is LiH₂PO₄ or LiPO₃, or Li₂O, LiOH, Li₂CO₃ or any other lithium compound that produces no byproducts which degrade the main product.
29. A process for the production of lithium metal phosphate/carbon nanocomposites according to claim 26, in which the phosphate precursor for lithium metal phosphate is LiH₂PO₄ or LiPO₃, NH₄H₂PO₄, phosphoric acid (HPO₃ or H₃PO₄), or any phosphate compound that produces no byproducts which degrade the main product.

30. A process for the production of lithium metal phosphate/carbon nanocomposites according to claim 27, in which the metal precursors for lithium metal phosphate are added in stoichiometric excess with respect to the phosphate precursor in order to favor formation of a metal oxide bonding layer (C-O-M) between carbon and lithium metal phosphate.
31. A process for the production of lithium metal phosphate/carbon nanocomposites according to claim 29, in which the phosphate precursor for lithium metal phosphate is added in stoichiometric excess with respect to the metal precursor in order to favor formation of a phosphate bonding layer (C-O-P) between carbon and lithium metal phosphate.
32. A process for the production of lithium metal phosphate/carbon nanocomposites according to claim 26 to 31, in which the carbon material is a high surface area electro-conductive carbon black, such as Printex XE 2 (Degussa), Black Pearls 2000 (Cabot) or Ketjenblack EC-300J or EC-600JD (Akzo Nobel).
33. A process for the production of lithium metal phosphate/carbon nanocomposites according to claim 26 to 31, in which the carbon material is single or multi walled carbon nanotubes (SWCNT or MWCNT).
34. A process for the production of lithium metal phosphate/carbon nanocomposites according to claim 26 to 31, in which the carbon material is natural or synthetic graphite, such as high surface graphite Timrex HSAG300 (Timcal), Timrex KS4 or KS 6 or KS44 graphite (Timcal), Timrex SFG6 or SFG44 graphite (Timcal), or Timrex MB 15 graphite (Timcal).
35. A process for the production of lithium metal phosphate/carbon nanocomposites according to claim 26 to 31, in which the carbon material is expanded graphite.
36. A process for the production of lithium metal phosphate/carbon nanocomposites according to claim 26 to 31, in which the carbon material is exfoliated graphite or graphite oxide or graphene.

37. A process for the production of lithium metal phosphate/carbon nanocomposites according to claim 26 to 36, in which milling is carried out in a ball mill, shaker mill, vibration mill, roller mill, attrition mill, jet mill or any other suitable mill.
- 5 38. A process for the production of lithium metal phosphate/carbon nanocomposites according to claim 26 to 37, in which milling is carried out under air or inert gas atmosphere, preferably in dry conditions or alternatively in the presence of a solvent.
- 10 39. A process for the production of lithium metal phosphate/carbon nanocomposites according to claim 26 to 38, in which the product of milling is heated for crystallization to 300-600⁰C, preferably to 400-500⁰C, for a sufficient time.
- 15 40. A process for the production of lithium metal phosphate/carbon nanocomposites according to claim 39, in which heat treatment is carried out under vacuum or inert gas atmosphere, such as nitrogen or argon, with or without addition of reducing gases, such as hydrogen or carbon monoxide/dioxide mixtures, or just under the exclusion of oxygen excess from the atmosphere.
- 20 41. A rechargeable battery comprising a cathode, an anode and an electrolyte, said cathode comprising a metal phosphate/carbon nanocomposite according to claims 1 to **40**.
- 25 42. A rechargeable battery according to claim 41, wherein the cathode further comprises a conductive additive.
43. A rechargeable battery according to claim 41, wherein the cathode further comprises a polymeric binder.

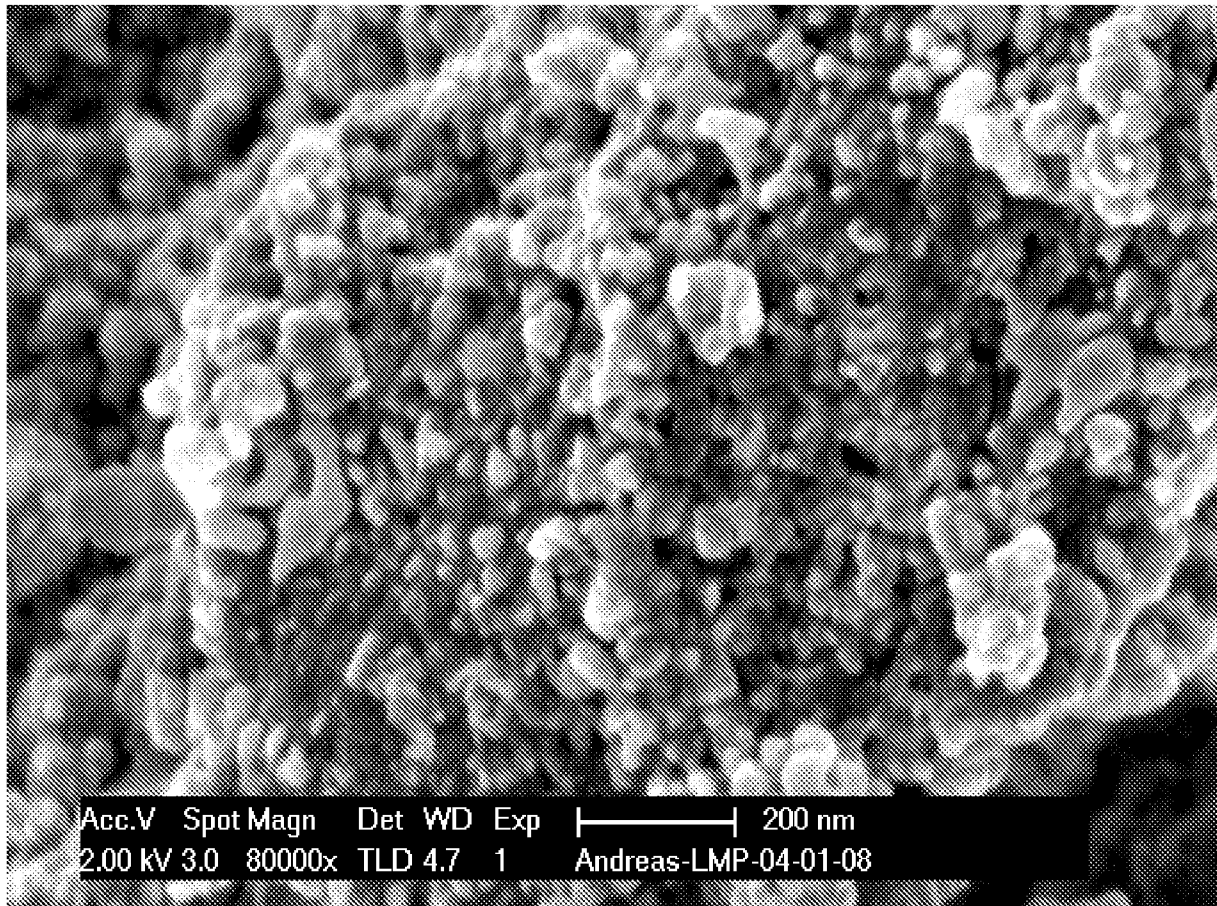


Figure 1

SEM picture of LiMn_{0.9}Fe_{0.1}PO₄/C nanocomposite (18% Ketjenblack EC600JD) after heating for 1 hour under argon/8% hydrogen at 450°C

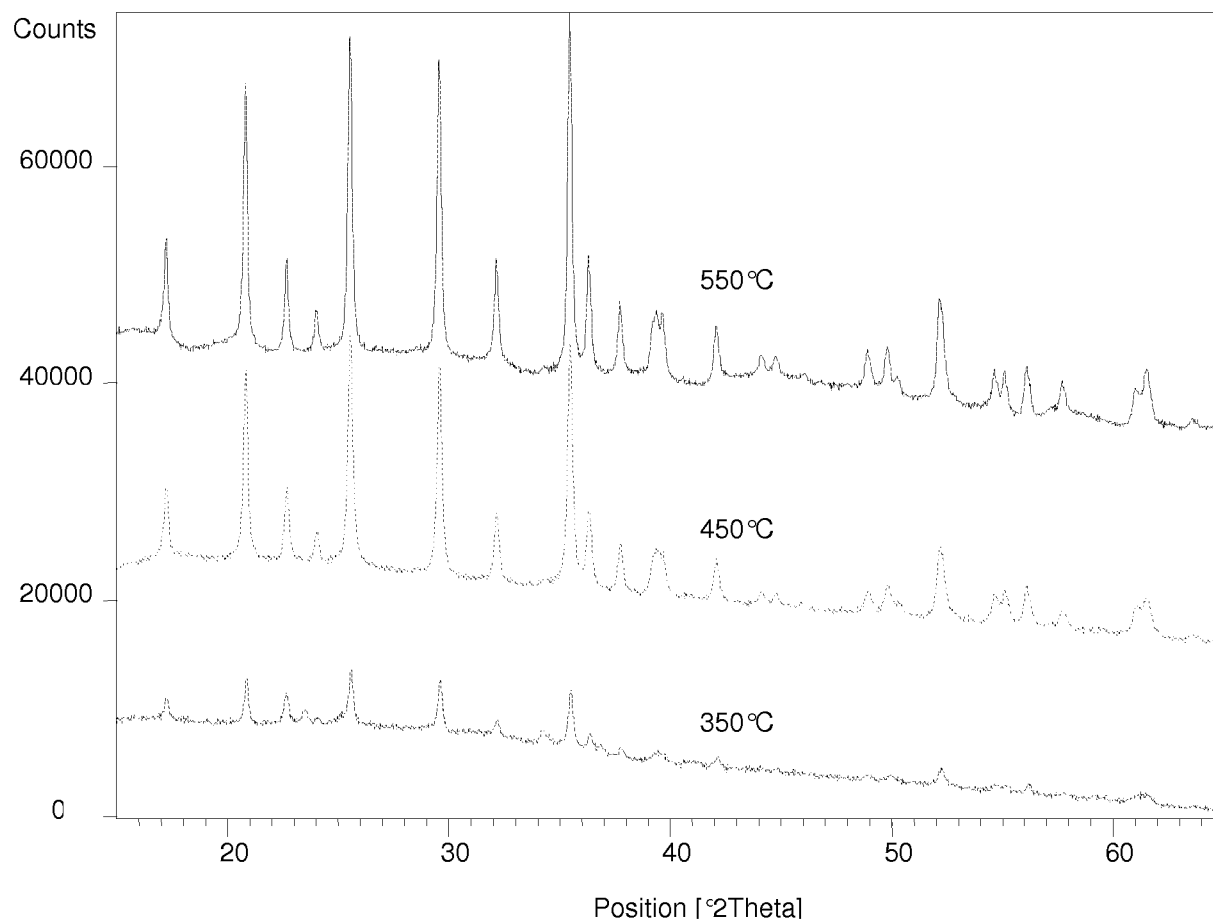


Figure 2

XRD patterns of $\text{LiMn}_{0.9}\text{Fe}_{0.1}\text{PO}_4/\text{C}$ nanocomposite (18% Ketjenblack EC600JD) after heating for 1 hour under argon/8% hydrogen at different temperatures

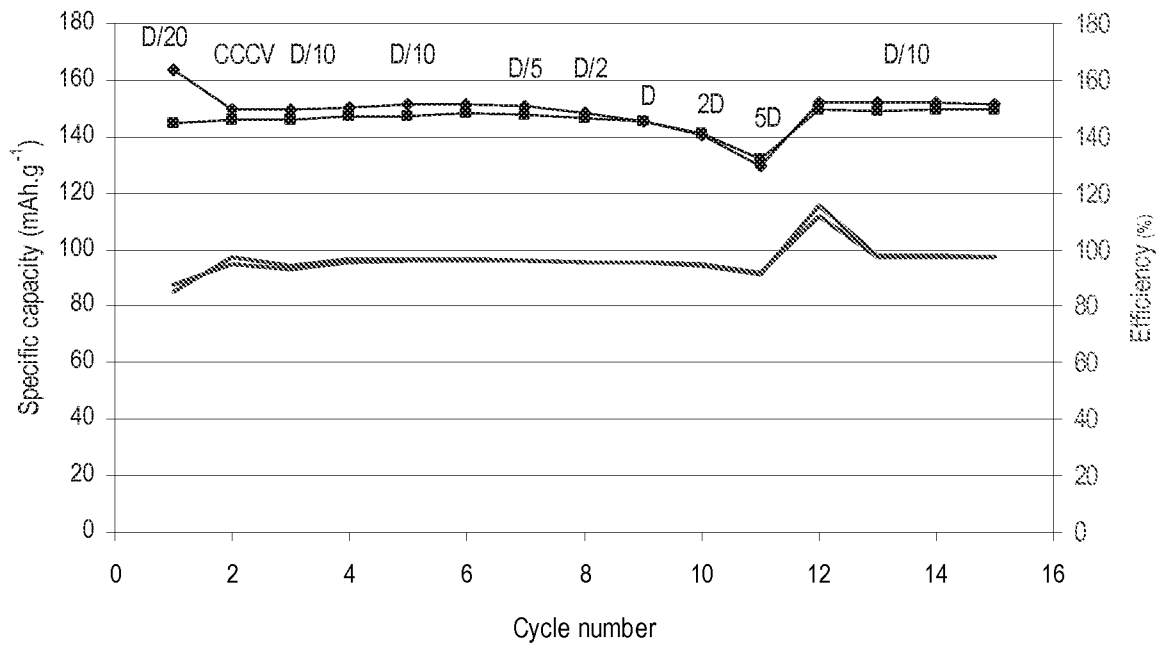


Figure 3

Electrochemical performance of two lithium batteries with $\text{LiMn}_{0.9}\text{Fe}_{0.1}\text{PO}_4/\text{C}$ nanocomposite cathode (18% Ketjenblack EC600JD) at different discharge rates

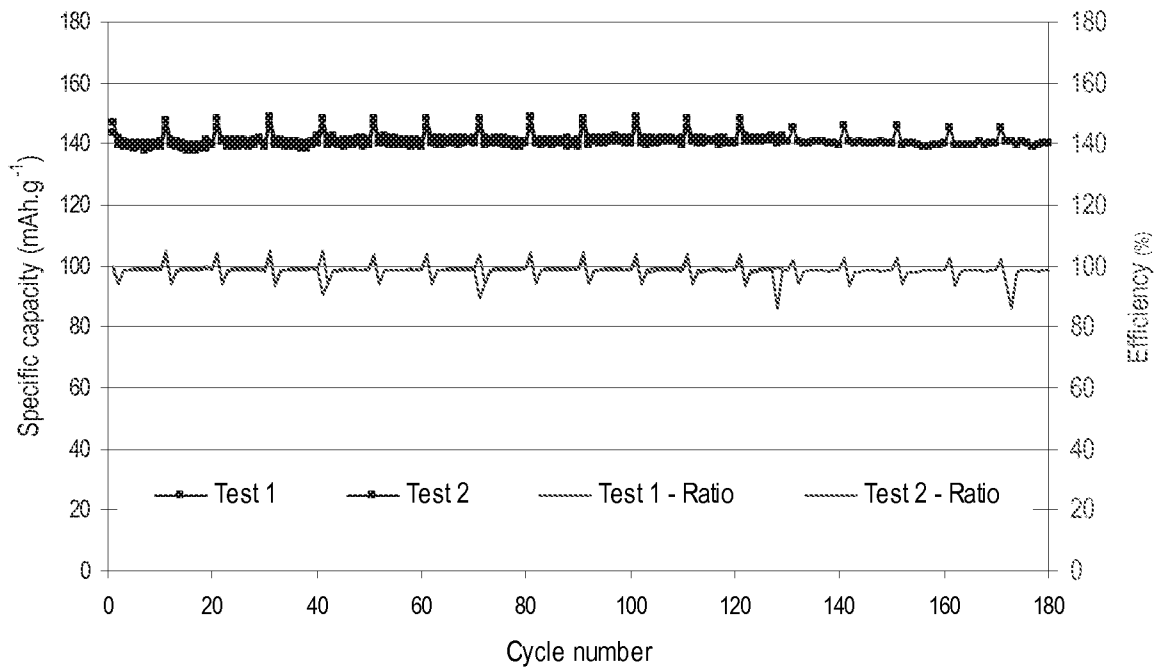


Figure 4

Cycling stability (at 1 C and C/10 each 10th cycle, charged up to 4.25 V) of two lithium batteries with $\text{LiMn}_{0.9}\text{Fe}_{0.1}\text{PO}_4/\text{C}$ nanocomposite cathode (18% Ketjenblack EC600JD)

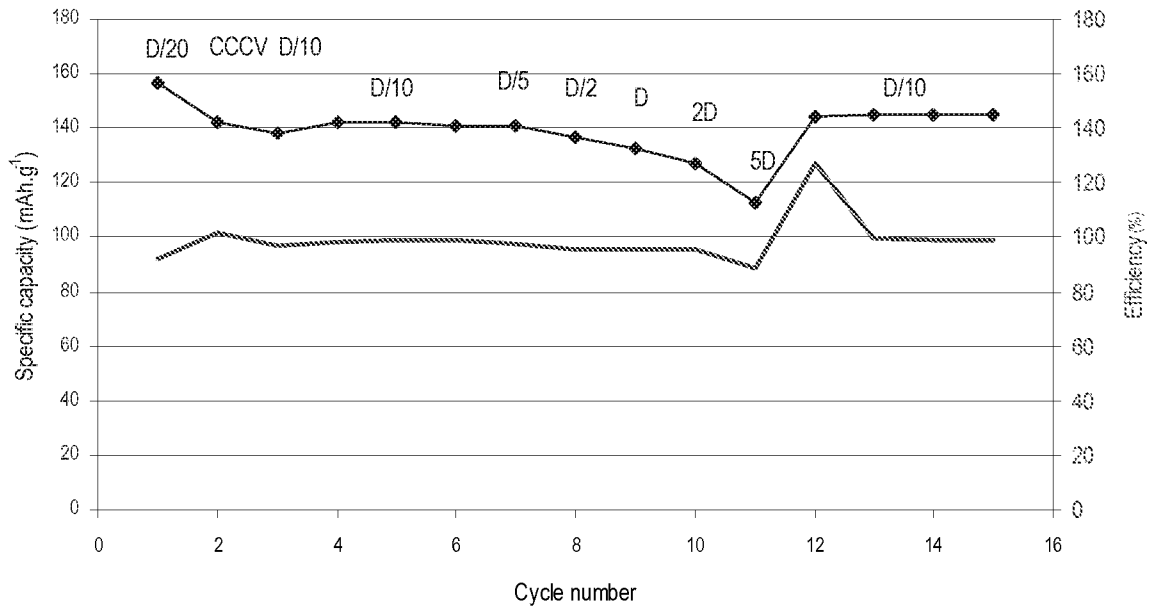


Figure 5

Electrochemical performance of lithium battery with $\text{LiMn}_{0.8}\text{Fe}_{0.2}\text{PO}_4/\text{C}$ nanocomposite cathode (10% Ketjenblack EC600JD) at different discharge rates

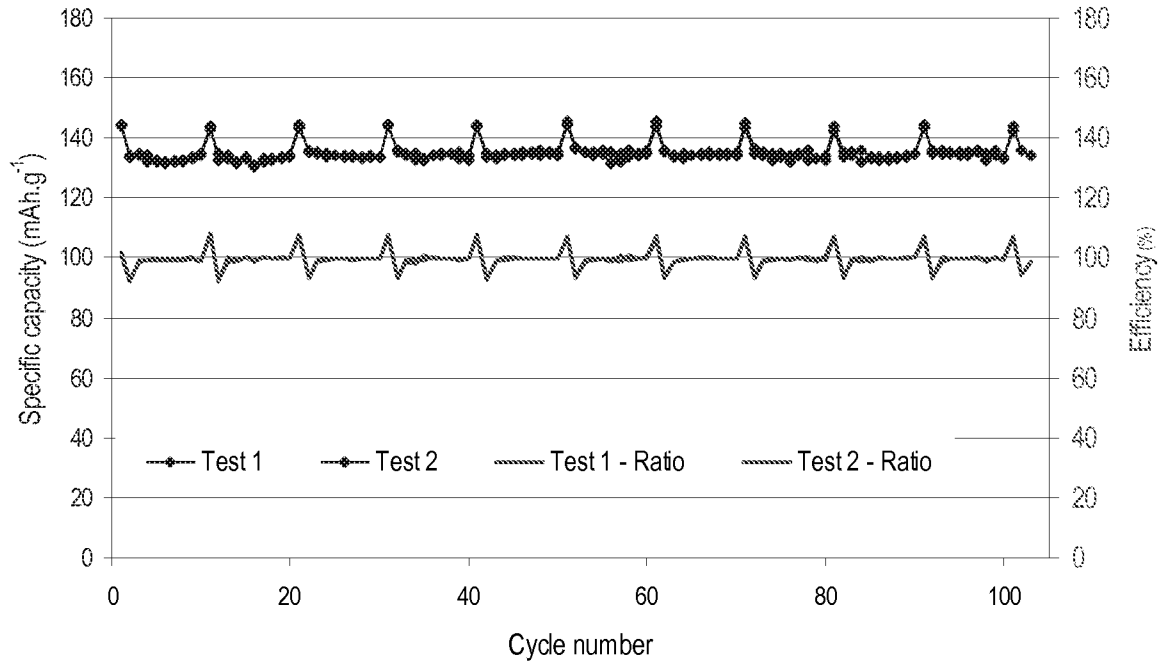


Figure 6

Cycling stability (at 1 C and C/10 each 10th cycle, charged up to 4.25 V) of two lithium batteries with $\text{LiMn}_{0.8}\text{Fe}_{0.2}\text{PO}_4/\text{C}$ nanocomposite cathode (10% Ketjenblack EC600JD)

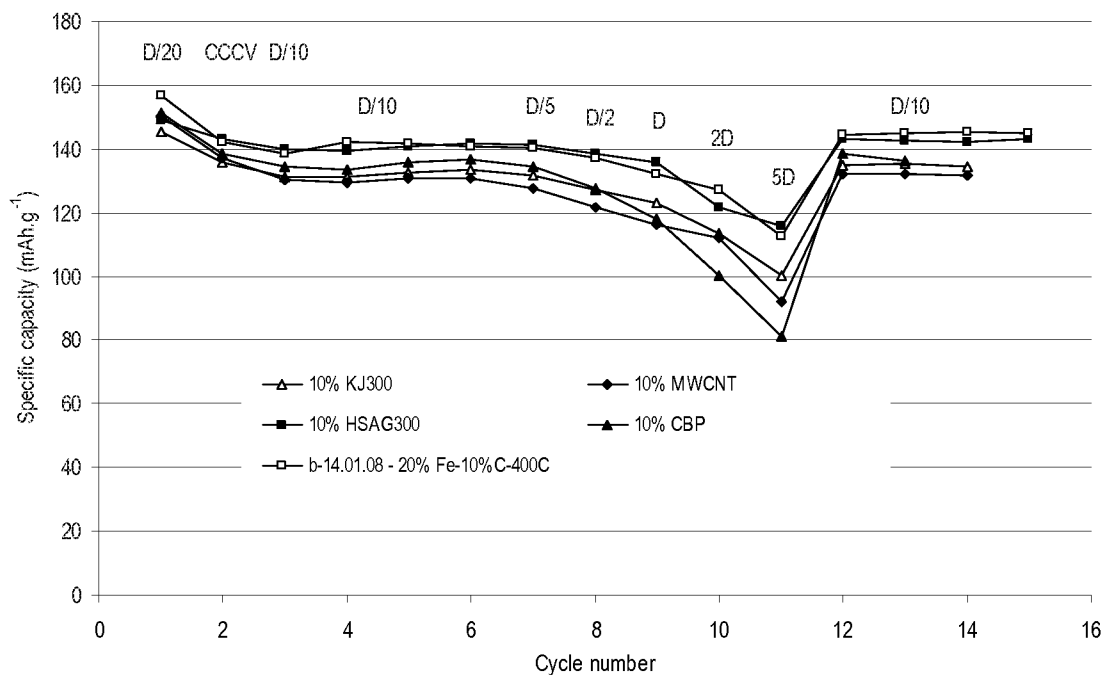


Figure 7

Electrochemical performance of lithium batteries with $\text{LiMn}_{0.8}\text{Fe}_{0.2}\text{PO}_4/10\% \text{C}$ nanocomposite cathodes prepared from different carbon sources:

△ Ketjenblack EC-300J (Akzo Nobel, 800 m^2/g)

□ Ketjenblack EC-600JD (Akzo Nobel, 1400 m^2/g)

▲ Black Pearls 2000 (Cabot, 1500 m^2/g)

◆ Multi walled carbon nanotubes (MWCNT)

■ High surface graphite Timrex HSAG300 (Timcal, 280 m^2/g)

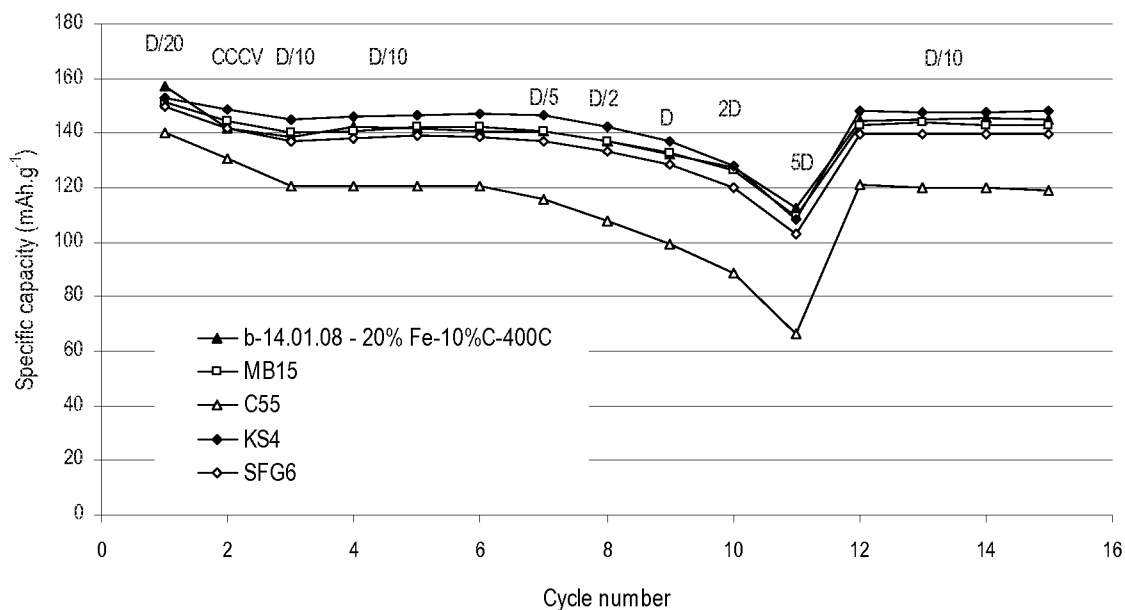


Figure 8

Electrochemical performance of lithium batteries with $\text{LiMn}_{0.8}\text{Fe}_{0.2}\text{PO}_4/10\%C$ nanocomposite cathodes prepared from different carbon sources:

- ▲ Ketjenblack EC-600JD (Akzo Nobel, $1400 \text{ m}^2/\text{g}$)
- ◆ Timrex KS4 graphite (Timcal, $26 \text{ m}^2/\text{g}$)
- ◇ Timrex SFG6 graphite (Timcal, $17 \text{ m}^2/\text{g}$)
- Timrex MB15 graphite (Timcal, $9.5 \text{ m}^2/\text{g}$)
- △ Shawinigan acetylene black C-55 ($70 \text{ m}^2/\text{g}$)

INTERNATIONAL SEARCH REPORT

International application No
PCT/IB2008/051418

A. CLASSIFICATION OF SUBJECT MATTER
 INV. C01B25/37 C01B25/45 H01M4/62

According to International Patent Classification (IPC) or to both national classification and IPC

B. FIELDS SEARCHED
 Minimum documentation searched (classification system followed by classification symbols)
COIB

Documentation searched other than minimum documentation to the extent that such documents are included in the fields searched

Electronic data base consulted during the international search (name of data base and, where practical, search terms used)
 EPO-Internal, WPI Data, INSPEC, COMPENDEX, CHEM ABS Data

C. DOCUMENTS CONSIDERED TO BE RELEVANT

Category*	Citation of document, with indication, where appropriate, of the relevant passages	Relevant to claim No.
X	LEI WANG ET AL: "Nano-LiFeP04/MWCNT cathode -materials prepared by room-temperature solid-state reaction and microwave heating" JOURNAL OF THE ELECTROCHEMICAL SOCIETY ELECTROCHEMICAL SOCIETY INC. USA, vol. 154, no. 11, November 2007 (2007-11), pages A1015-A1019, XP002513827 ISSN: 0013-4651 the whole document <div style="text-align: center;">----- -/--</div>	1-38, 41-43

Further documents are listed in the continuation of Box C. See patent family annex.

* Special categories of cited documents :

<p>"A¹" document defining the general state of the art which is not considered to be of particular relevance</p> <p>"E" earlier document but published on or after the international filing date</p> <p>"L¹" document which may throw doubts on priority claim(s) <small>over</small> which is cited to establish the publication date of another citation or other special reason (as specified)</p> <p>"O" document referring to an oral disclosure, use, exhibition or other means</p> <p>"P" document published prior to the international filing date but later than the priority date claimed</p>	<p>"T" later document published after the international filing date or priority date and not in conflict with the application but cited to understand the principle <i>or</i> theory underlying the invention</p> <p>"X" document of particular relevance; the claimed invention cannot be considered novel or cannot be considered to involve an inventive step when the document is taken alone</p> <p>"Y¹" document of particular relevance; the claimed invention cannot be considered to involve an inventive step when the document is combined with one or more other such documents, such combination being obvious to a person skilled in the art.</p> <p>"&" document member of the same patent family</p>
---	---

Date of the actual completion of the International search 6 February 2009	Date of mailing of the international search report 17/02/2009
--	--

Name and mailing address of the ISA/ European Patent Office, P.B. 5818 Patentlaan 2 NL - 2280 HV Rijswijk Tel. (+31-70) 340-2040, Fax: (+31-70) 340-3016	Authorized officer Rigondaud, Bernard
--	---

INTERNATIONAL SEARCH REPORT

International application No
PCT/IB2008/051418

C(Continuation). DOCUMENTS CONSIDERED TO BE RELEVANT		
Category*	Citation of document, with indication, where appropriate, of the relevant passages	Relevant to claim No
X	DATABASE CA [On line] CHEMICAL ABSTRACTS SERVICE, COLUMBUS, OHIO, US; MIYAYAMA, MASARU ET AL: "Secondary lithium batteries, and their cathodes, and preparation of same cathodes" XP002513895 retrieved from STN Database accessi on no. 142: 433160 abstract	1,25, 41-43
A	& JP 2005 123107 A (HITACHI MAXELL LTD., JAPAN) 12 May 2005 (2005-05-12) -----	26, 32-36
X	DATABASE WPI Week 2008 Thomson Scientific, London, GB; AN 2008-N02991 XP002513896 & CN 101 081 696 A (SHENGZHEN BEITERUI ELECTRONIC MATERIAL CO LTD) 5 December 2007 (2007-12-05) abstract -----	1,26-34, 41-43
X	CHEN J ET AL: "Hydrothermal synthesi s of lithium iron phosphate" ELECTROCHEMISTRY COMMUNICATIONS MAY 2006 ELSEVIER INC. US, vol . 8, no. 5, May 2006 (2006-05) , pages 855-858, XP002513828 -----	1,25 , 41-43
A	-----	26, 33
X	EP 1 195 837 A (SONY CORP [JP]) 10 April 2002 (2002-04-10) c l a i m s 1,7,8 paragraphs [0022] - [0028] paragraphs [0032] - [0075] paragraphs [0084] , [0085] examples 1,5-8, 13, 14,16, 17	1,23, 25-29, 37-43
A	-----	2-22,24
X	& US 7 122 272 B2 (OKAWA TSUYOSHI [JP] ET AL) 17 October 2006 (2006-10-17) cited in the appl icati on -----	1,23, 25-29, 37-43
X	EP 1 184 920 A (SONY CORP [JP]) 6 March 2002 (2002-03-06) cited in the appl icati on c l a i m s 3,7,8, 10 paragraphs [0049] - [0053] paragraph [0059] paragraph [0063] paragraph [0065] example 1	1,23, 26-29, 37-40
A	-----	1

INTERNATIONAL SEARCH REPORT

Information on patent family members

International application No PCT/IB2008/051418
--

Patent document cited in search report	Publication date	Patent family member(s)	Publication date
JP 2005123107	A	12-05-2005	NONE
<hr/>			
CN 101081696	A	05-12-2007	NONE
<hr/>			
EP 1195837	A	10-04-2002	CA 2358281 AI 06-04-2002
		CN 1350342 A	22-05-2002
		JP 3988374 B2	10-10-2007
		JP 2002117907 A	19-04-2002
		KR 20020027287 A	13-04-2002
		MX PA01009976 A	20-08-2003
		TW 541739 B	11-07-2003
		US 2002106563 AI	08-08-2002
<hr/>			
US 7122272	B2	17-10-2006	CA 2358281 AI 06-04-2002
		CN 1350342 A	22-05-2002
		EP 1195837 A2	10-04-2002
		JP 3988374 B2	10-10-2007
		JP 2002117907 A	19-04-2002
		KR 20020027287 A	13-04-2002
		MX PA01009976 A	20-08-2003
		TW 541739 B	11-07-2003
		US 2002106563 AI	08-08-2002
<hr/>			
EP 1184920	A	06-03-2002	CN 1340869 A 20-03-2002
		JP 4151210 B2	17-09-2008
		JP 2002075364 A	15-03-2002
		KR 20020018093 A	07-03-2002
		MX PA01008733 A	12-08-2004
		TW 518785 B	21-01-2003
		US 2002047112 AI	25-04-2002
<hr/>			